13th World Conference on Earthquake Engineering
Vancouver, B.C., Canada
August 1-6, 2004
Paper No. 618

SOURCE MODELING USING CIRCULAR CRACK BY A WAVEFORM INVERSION

Tomoki HIKITA[1], Tomonori IKEURA[2]

SUMMARY

Forward directivity of strong ground motions is one of the main sources of large velocity pulses that can cause great damage to flexible buildings. Methods for evaluating the duration and amplitude of such pulses are very important in engineering design. The circular crack model can characterize the rupture propagation on a fault and evaluate the near-fault pulses, but needs to express the rupture propagation more applicably. In this study, a circular crack model is proposed, which can systematically express various states of the rupture propagation on a fault. We applied the proposed model to estimate the specific crack model and to characterize the rupture propagation on a fault, for the 1997 Yamaguchi, Japan, earthquake. The estimated crack model can effectively simulate the near-fault velocity pulses and the calculated waveforms match the observed waveforms in the period range from 1s to 10s.

INTRODUCTION

The longer period (>1s) near-fault ground motions of large earthquakes have been simulated successfully in recent works (e.g., Wald [1], Yoshida [2]). It has been understood that forward directivity is one of the main causes of velocity pulses observed in near-fault regions. The near-fault strong ground motions containing large velocity pulses could potentially cause great damage to flexible buildings. Evaluation of the duration and amplitude of such pulses have great importance in engineering design at near fault sites.

A large number of strong ground motion records has recently enabled us to analyze more precisely the characteristics of near-fault ground motions, and to examine methods for evaluating near-fault pulses (e.g., Alavi [3], Mavroeidis [4]). These methods are purely phenomenological, so we still need to develop analytical models based on physical understandings of near-fault pulse generation. An analytical models needs to be simple, yet effective in simulating near-fault strong ground motions. Campillo [5] simulated near-fault ground motions recorded at the Caleta de Campos station during the 1985 Michoacan, Mexico, earthquake using simple asymmetrical crack model. A crack model seems to be able to characterize the rupture propagation on a fault providing it is aimed at simulating long period pulses, but it is not confirmed that near-fault pulses due to various earthquakes can be successfully simulated using a crack

[1] Research Engineer, Kajima Technical Research Institute, Tokyo, Japan.
[2] Supervisory Research Engineer, Kajima Technical Research Institute, Tokyo, Japan.

model. To apply a crack model to simulating near-fault pulses due to various earthquakes, a crack model needs to be able to express asymmetrical and symmetrical rupture propagation systematically.

In this study, we propose a circular crack model that can systematically express various states of the rupture propagation, and a method for characterizing the rupture propagation on the fault during an actual earthquake using the proposed model. By applying the method, we derive a specific crack model for the 1997 Yamaguchi, Japan, earthquake in which the waveforms calculated by the model best match with the observed waveforms in the period range from 1s to 10s.

SOURCE MODEL

From our point of view, the source model needs to be simple, yet effective in simulating near-fault strong ground motions. Sato [6] proposed a simple shear crack model in which the rupture nucleates at the center of the crack, grows radially at a constant rupture velocity, and stops abruptly at a specified radius. Dong [7] proposed an asymmetrical circular crack model in which the rupture starts at a point on the edge of the circular crack, and exhibits unidirectional propagation. As intuitively expected, the radiation of the latter model exhibits a dependence on azimuth and stronger directivity effects than the former model. From our perspective, the source model for simulating strong ground motions of an arbitrary earthquake should be able to approximate various rapture propagations systematically. Therefore, we proposed a circular crack model that has this possibility.

The rupture growth of our proposed crack model is shown in Figure 1. The rupture starts at a point *O* inside the circular crack and grows radially so that at any time instant the center of the expanding radial crack moves at a constant velocity on a diameter passing through point *O*. Stopping of slip occurs simultaneously over the entire surface of the crack when the rupture front stumbles at the edge of the crack. The slip at any time instance is specified by the static solution of the circular crack (Eshelby [8]). In this model, the distance between the point where rupture starts and the center of the crack is expressed as $\alpha\rho_0$, where ρ_0 is the crack radius, and α is a coefficient that takes a value of 0 to 1. For α=0, the rupture starts at the center of the crack, and the model is equivalent to that proposed by Sato [6]. For α=1, the rupture starts at a point on the edge of the crack, and the model is equivalent to that proposed by Dong [7].

Defining a polar coordinate system as shown in Figure 1, the slip time function of this model is given by:

$$u(\rho,\phi,t)=\begin{cases} K\sqrt{\left(\dfrac{1-\alpha}{1+\alpha}\right)v_r^{\,2}t^2+\left(\dfrac{2\alpha}{1+\alpha}\right)\rho v_r t\cos\phi-\rho^2}\; H\left(t-\dfrac{\rho(1+\alpha)}{v_r Z}\right)\left[1-H(\rho-\rho_0 Z)\right] \quad , \quad v_r t<(1+\alpha)\rho_0 \\[2ex] K\sqrt{(1-\alpha^2)\rho_0^{\,2}-\rho^2+2\alpha\rho\rho_0\cos\phi}\;\left[1-H(\rho-\rho_0 Z)\right] \quad , \quad v_r t>(1+\alpha)\rho_0 \end{cases}$$

where

$$Z=\sqrt{1-\alpha^2\sin^2\phi}+\alpha\cos\phi\,,$$

$H(t)$ is the Heaviside unit step function, $K=(24/7\pi)(\Delta\sigma/\mu)$, $\Delta\sigma$ is the stress drop, μ is the rigidity of the medium, and v_r is the constant rupture velocity. The slip function at various locations of the crack is shown in Figure 2.

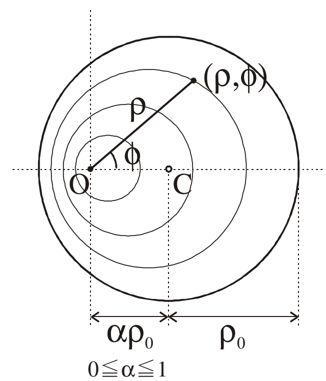

Fig 1. Rupture growth of the proposed crack model. The rupture starts at a point *O* of a crack centered at point *C*. The starting point can be assigned at any point on the crack according to the specification of a coefficient α.

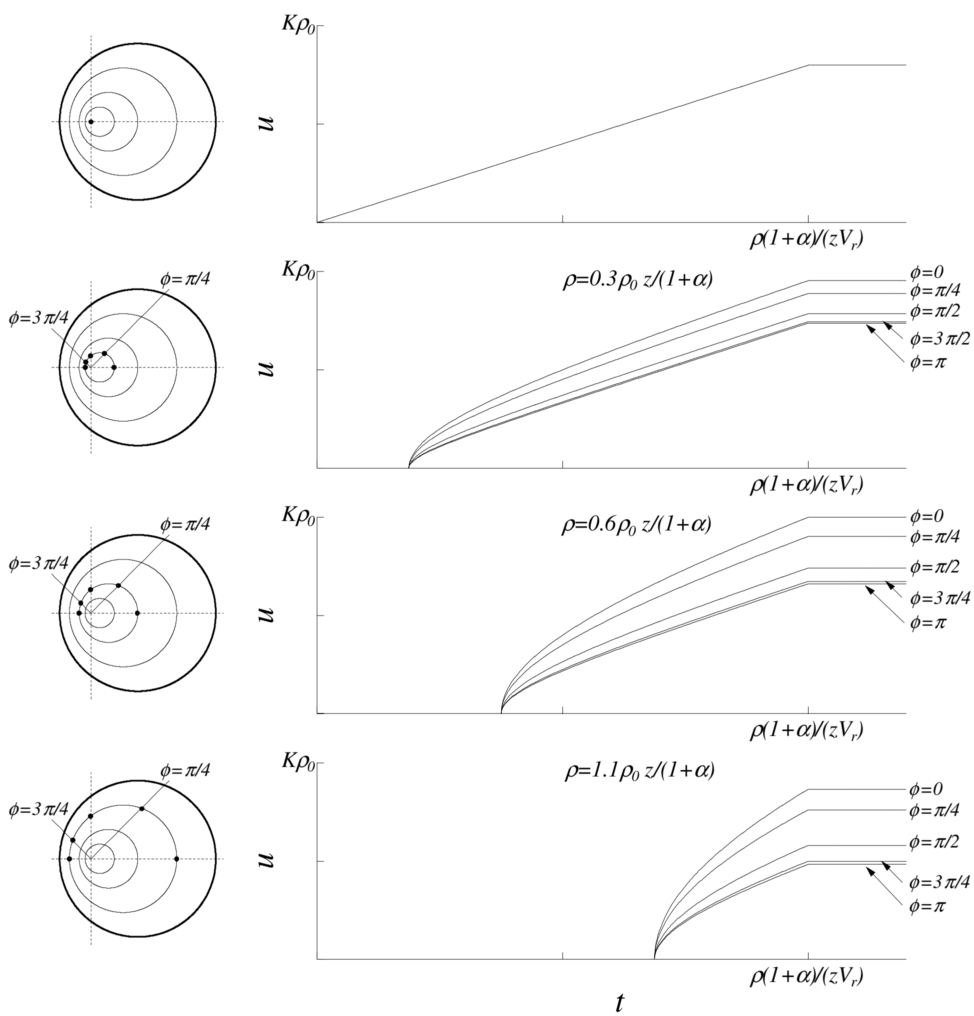

Fig 2. Slip functions of the proposed crack model at selected points (indicated with dots). The abscissa represents absolute time *t*. The amplitude $K\rho_0$ denotes the final slip at a center of the crack.

SYNTHESIZED GROUND MOTIONS

The n-direction displacement at the location $\mathbf{x}$ due to general displacement discontinuity across the faulting surface Σ is represented as follows (Aki [9])

$$U_n(\mathbf{x},t) = \iint_{\Sigma} m_{pq}(\xi,\tau) * G_{np,q}(\mathbf{x},t;\xi,\tau)\, d\Sigma$$

with

$$m_{pq}(\xi,\tau) = [u_i]\, v_j c_{ijpq}$$

where $G_{np,q}(\mathbf{x},t;\xi,\tau)$ is the spatial derivative of the Green's function tensor representing an n-direction displacement response at $\mathbf{x}$ to a p-direction unit dislocation on a plane normal to the q-direction at ξ, $m_{pq}(\xi,\tau)$ is the moment-density tensor corresponding to the slip $[u_i]$, v_j is the vector normal to Σ, c_{ijpq} is the elastic constant tensor of Hooke's law, and the symbol * represents the convolution. For numerical integration of the equation, we replace the integral by a summation over grid points. When the crack radius is much smaller than the distance between a reference point (the center of the crack) and a station, the Green's function from an arbitrary point ξ on the crack to the station approximates that from the reference point after correcting for the time delay owing to the difference of location. Therefore, the approximation expressed as follows is taken into the numerical integration.

$$G_{np,q}(\mathbf{x},t;\xi,\tau) \cong G_{np,q}(\mathbf{x},t-t_d;\mathbf{o},\tau)$$

with

$$t_d = \frac{1}{c}\left(\frac{\xi\mathbf{x}}{R}\right)$$

where $\mathbf{o}$ is a reference point on the crack, R is the distance between the reference point and the station, and c is the S-wave velocity at the source location (because our main target is the direct S-wave). Practically, multiple reference points are considered when the crack radius is larger.

Figure 3 shows examples of the velocity waveforms at selected stations from the artificial crack in an elastic half-space. The rupture starts at a point on the edge of the crack (α=1). The waveforms are calculated in the period range longer than 1s. The assumed parameters of the medium, the rupture velocity, and the stress drop are shown in Fig 3. The large velocity pulse due to the forward directivity excels in Y-component velocity waveform at station 1. The apparent phase of the X-component at station 3 corresponds to the stopping phase.

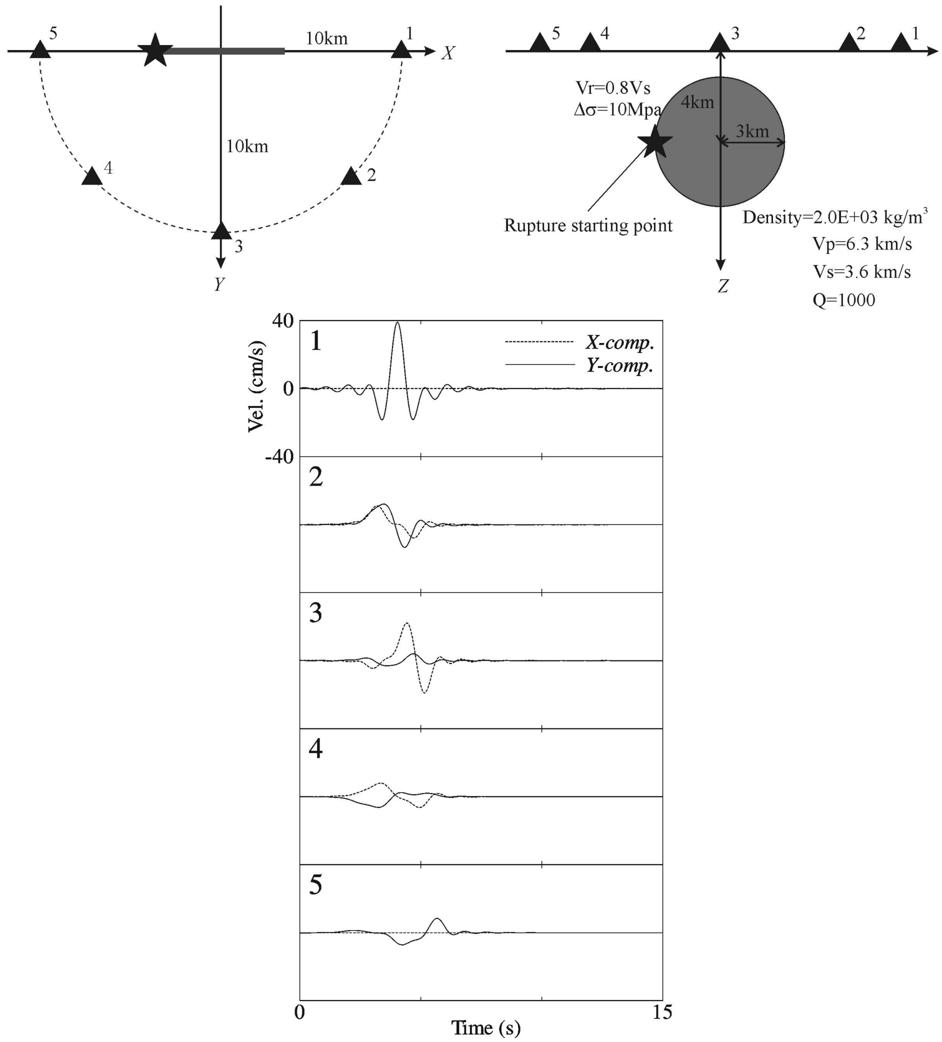

Fig 3. The velocity waveforms at 5 stations calculated from an artificial crack in an elastic half-space. The rupture starts at a point on the edge of the crack (α=1). The waveforms are calculated in the period range longer than 1s.

INVERSION METHOD

Our objective is to find a specific crack model that the waveforms calculated by the model best match with the observed waveforms in the period range from 1s to 10s. By using the proposed crack model, the model is represented by 1) a location on the assumed fault plane, 2) a radius, 3) a stress drop, 4) a rake angle, 5) a rupture propagation velocity inside the crack, 6) a rupture starting time, 7) a rupture starting point on the crack, and 8) the number of cracks. These parameters are estimated by the waveform inversion using the very fast simulated annealing (VFSA, Ingber [10]), because the inverse problem of our analysis is highly nonlinear and its convergence properties are not known. The algorithm iterates by updating the parameters so that the misfit function defined as follows becomes less, and repeats the process until the parameters converge.

The misfit function corresponding to the *i*th model m_i is defined as

$$E(m_i) = \frac{1}{N} \sum_{l=1}^{N} \left(\frac{\sum_k \left(W_k^S - W_k^O\right)^2}{\sum_k \left(W_k^O\right)^2} \right)$$

where N is a product of number of stations and number of components, W_k^O and W_k^S are kth data of the observed waveform converted to velocity and that of the corresponding simulated velocity waveform, respectively.

In our analysis, the rupture propagation velocity inside the crack is assumed to be 80 percent of the *S*-wave velocity. The number of cracks is determined a priori, referring to the number of apparent pulses in the near-fault strong motion records. When the simulated waveform does not match well enough with observed waveform, a re-estimation using a plural number of cracks is carried out.

INVERSION OF THE 1997 YAMAGUCHI, JAPAN, EARTHQUAKE

The Yamaguchi earthquake (Mw 5.9) occurred on June 25, 1997 in northern Yamaguchi prefecture, Japan. This was one of the largest inland earthquakes that occurred in Japan since the installation of the Kyoshin Net (K-NET) in 1996, the network of strong motion seismometers installed by the National Research Institute for Earth Science and Disaster Prevention (NIED) (Kinoshita [11]). Figure 4 shows the stations used in this study, the velocity waveforms in the period range from 1s to 10s at the stations, and the fault plane assumed by Ide [12]. The most apparent velocity pulse is observed at the station "SMN014" with a period of about 1.3s. The apparent pulse seems to be one, and the number of cracks is assumed to be one.

Green's functions for this study are calculated in a layered half-space by the discrete wave-number integral method by Hisada [13], assuming the structure of Table 1. The crack model characterizing the source process of the Yamaguchi earthquake is estimated by the aforementioned inversion procedure. We carry out the inversion for 5 cases with different randomness in VFSA to check the stability of the model calculated by our inversion procedure, and adopt the model that makes the misfit function least as the optimum model.

Figure 5 shows the estimated crack model, and Figure 6 shows the velocity waveform calculated by this model. The velocity waveform expresses the velocity pulses of observed records well. The estimated crack model effectively simulates the near-fault pulses. Figure 7 shows the results of 4 other cases of inversions. The estimated parameters (location, rupture starting point, moment, and rake angle) of the cracks are stable. The estimated crack model is compared with the source model of the Yamaguchi earthquake by Ide [12] in Figure 8. The location of the crack and the region with large slip in the model of Ide [12] are approximately correspondent.

Table 1.Velocity structure used in the analysis

Vp m/s	Vs m/s	Density kg/m^3	Depth m	Qp	Qs
5600	3230	2.50E+03	0	400	200
6000	3470	2.70E+03	3000	600	300
6600	3820	3.00E+03	16000	800	400
7800	4500	3.20E+03	30000	1000	500
8000	4620	3.25E+03	70000	1000	500

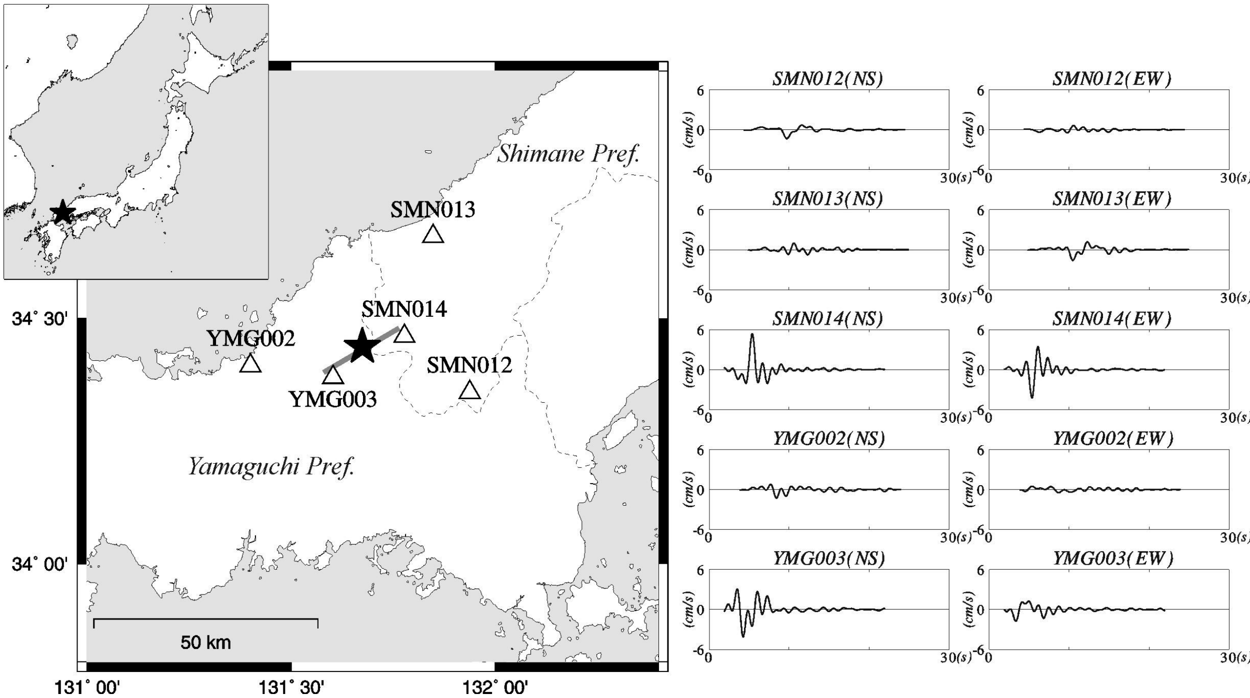

Fig 4. Location of the 1997 Yamaguchi earthquake (solid star), stations (open triangle) and the velocity waveforms in the period range from 1s to 10s. Thick line in the map shows the assumed fault plane (strike=-125deg., dip=86deg., length=16km, width=12km).

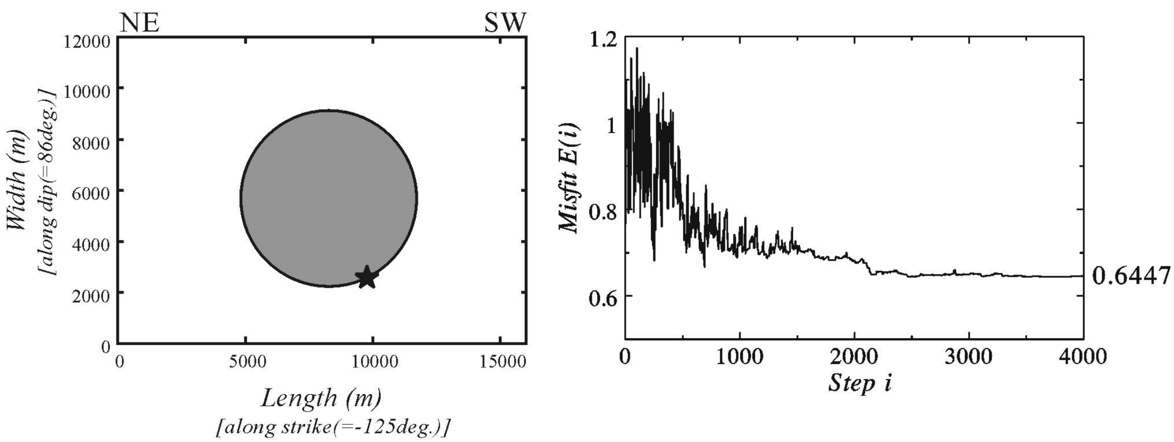

Location of a crack center (Length, Width)	(8291m, 5660m)
Radius	3479 m
Rake angle	-183.1 deg.
Time delay	0.0 s
Stress drop	2.4 MPa
Moment	2.35E+17 Nm (41%)*
Maximum slip	0.36 m

* The percentage for the total moment estimated by NIED.

Fig 5. Estimated circular crack (gray circle in figure of top left) on the assumed fault plane. Solid star shows the rupture starting point. The bottom table represents estimated parameters of the crack. The figure of top right shows the convergence of the misfit for the calculation.

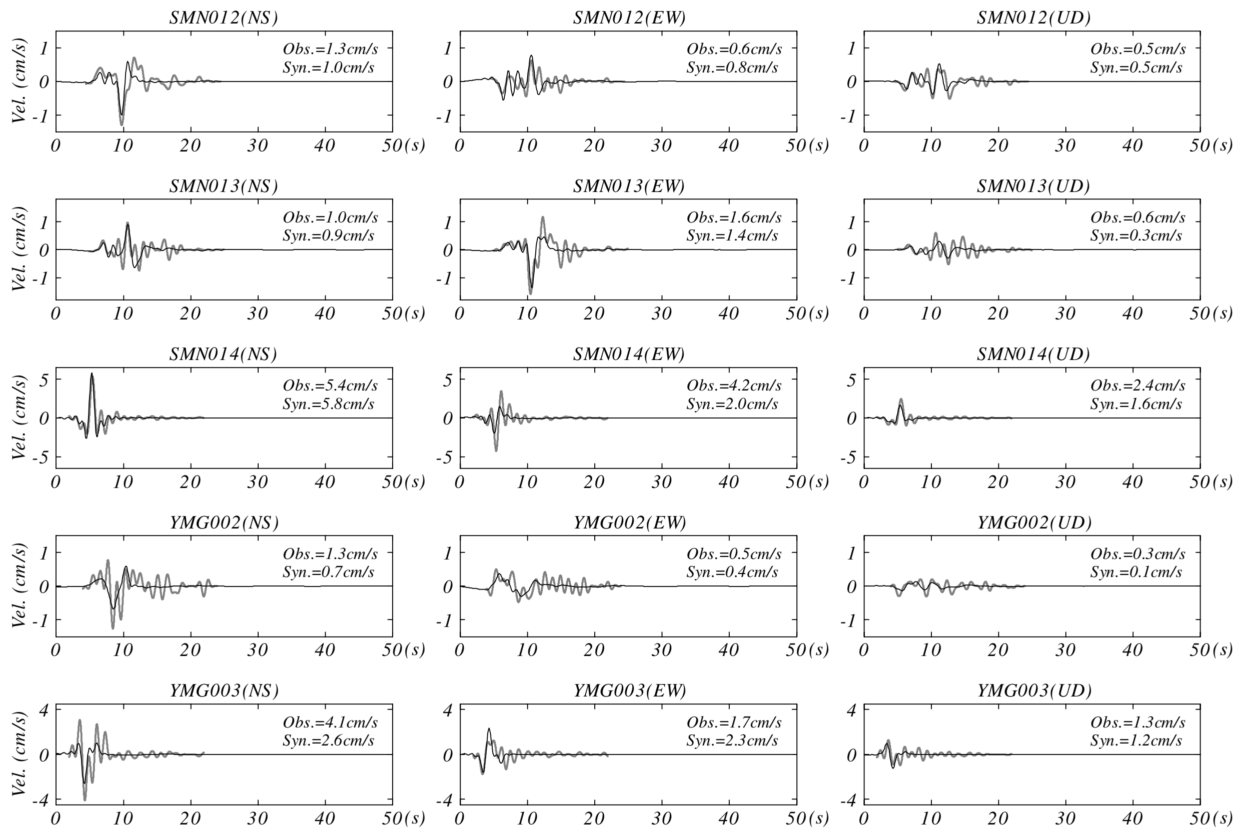

Fig 6. Synthetic velocity waveforms (black lines) and observed velocity waveforms (gray lines). The numbers at the top right corner of each box represent the maximum values in each trace.

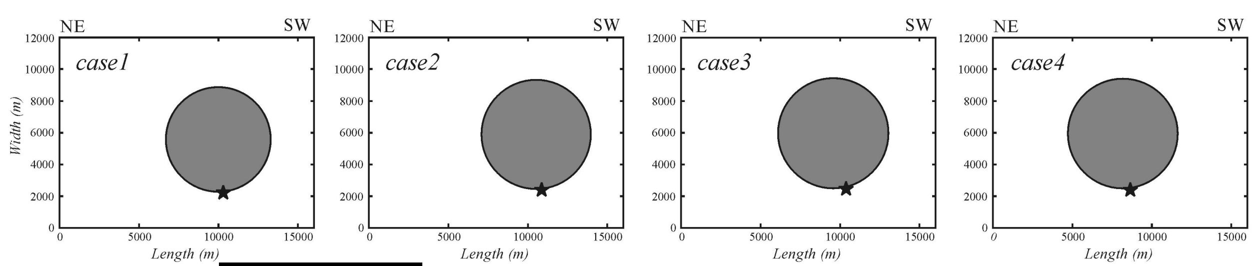

	Optimum model	case1	case2	case3	case4
Location	(8291m, 5660m)	(9940m, 5560m)	(10417m, 5891m)	(9471m, 5958m)	(10199m, 5936m)
Radius	3479 m	3325 m	3436 m	3472 m	3480 m
Rake angle	-183.1 deg.	-181.4 deg.	-182.6 deg.	-184.1 deg.	-181.3 deg.
Time delay	0.0 s	0.0 s	0.0 s	0.0 s	0.0 s
Stress drop	2.4 MPa	2.8 MPa	2.5 MPa	2.5 MPa	2.4 MPa
Moment	2.35E+17 Nm (41%)	2.33E+17 Nm (41%)	2.31E+17 Nm (41%)	2.35E+17 Nm (41%)	2.35E+17 Nm (41%)
Maximum slip	0.36 m	0.39 m	0.36 m	0.36 m	0.36 m
Misfit	0.6447	0.6454	0.6469	0.6453	0.6456

Fig 7. The results of 4 other cases of inversions. Bottom table represents the estimated parameters of each crack comparing with the optimum model (Fig 5). The moment and maximum slip are induced by the radius and stress drop.

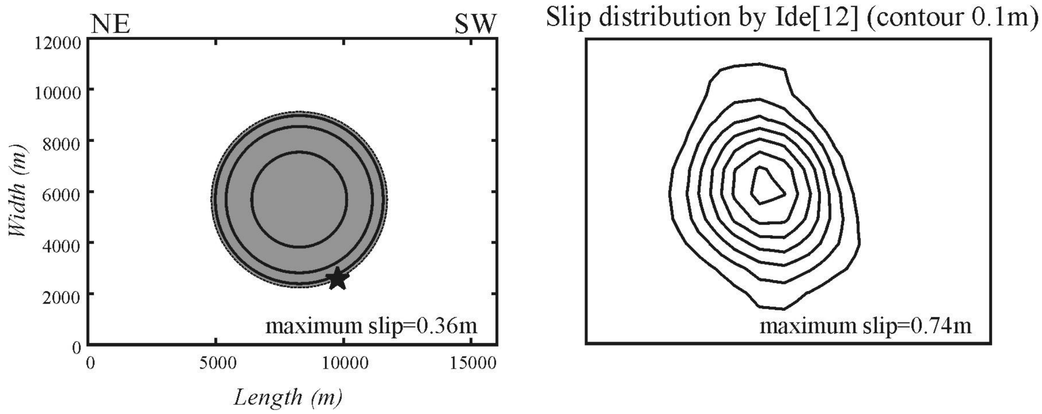

Fig 8. Comparison between estimated model (left) and source model estimated by Ide [12](right). Contour interval is 0.1m.

CONCLUSIONS

A crack model that can systematically express various states of the rupture propagation is proposed. The source process of the Yamaguchi earthquake is characterized using this crack model. The velocity waveform calculated by the estimated model successfully simulates the near-fault velocity pulses. The crack model estimated by our procedure effectively simulates the near-fault velocity pulses.

The estimation of the specific crack model of various earthquakes is important in predicting near-fault pulses for future earthquakes occurring on a causative fault. It is necessary to establish scaling laws for the parameters of the model (i.e., how a radius and a moment scale with earthquake size), and to investigate a characteristics of the location of the crack and the rupture propagation of various earthquakes.

However, the proposed method only describes coherent (long-period) components. There is generally a need to consider incoherent (high-frequency) components for engineering analysis and design. For example, one of the solutions is to hybridize the proposed method with a stochastic method (e.g., Mavroeidis [4]).

ACKNOWLEDGEMENTS

We thank Dr. Yoshiaki Hisada who provided us with FORTRAN codes to compute Green's functions for viscoelastic layered half-spaces. We also thank the National Research Institute for Earth Science and Disaster Prevention for providing the strong ground motion records (K-NET data). Some figures were made using a Generic Mapping Tool.

REFERENCES

1. Wald D. J., Heaton T. H., Hudnut K. W. "The slip history of the 1994 Northridge, California, earthquake determined from strong-motion, teleseismic, GPS, and leveling data." *Bull. Seism. Soc. Am.*, **86**, S49-S70, 1996.

2. Yoshida S., Koketsu K., Shibazaki B., Sagiya T. Kato T., Yoshida Y. "Joint inversion of near- and far-field waveforms and geodetic data for the rupture process of the 1995 Kobe earthquake." *J. Phys. Earth*, **44**, 437-454, 1996.
3. Alavi B., Krawinkler H. "Consideration of near-fault ground motion effects in seismic design." *Proc. of the 12th World Conf. Earthq. Eng.*, No.2665, 2000.
4. Mavroeidis G. P., Papageorgiou A. S. "A mathematical representation of near-fault ground motions." *Bull. Seism. Soc. Am.*, **93**, 1099-1131, 2003.
5. Campillo M., Gariel J. C., Aki K., Sanchez-Sesma F. J. "Destructive strong ground motion in Mexico city: source, path, and site effects during great 1985 Michoacan earthquake." *Bull. Seism. Soc. Am.*, **79**, 1718-1735, 1989.
6. Sato T., Hirasawa T. "Body wave spectra from propagating shear cracks." *J. Phys. Earth*, **21**, 415-431, 1973.
7. Dong G., Papageorgiou A. S. "Seismic radiation from a unidirectional asymmetrical circular crack model, Part I : Constant rupture velocity." *Bull. Seism. Soc. Am.*, **92**, 945-961, 2002.
8. Eshelby J. D. "The determination of the elastic field of an ellipsoidal inclusion and related problems." *Proc. Roy. Soc. London*, **A241**, 376-396, 1957.
9. Aki K., Richards P. G. "Quantitative seismology." W. H. Free-man, San Francisco, 1980.
10. Ingber L. "Very fast simulated re-annealing." *Mathl. Comput. Modelling*, **12**, 967-973, 1989.
11. Kinoshita S. "Kyoshin Net (K-NET)." *Seismol. Res. Lett.*, **69**, 309-332, 1998.
12. Ide S. "Source process of the 1997 Yamaguchi, Japan, earthquake analyzed in different frequency bands." *Geophys. Res. Lett.*, **26**, 1973-1976, 1999.
13. Hisada Y. "An efficient method for computing Green's functions for a layered half-space with sources and receivers at close depth (Part 2)." *Bull. Seism. Soc. Am.*, **85**, 1080-1093, 1995.